Supporting Information

Tuning band gap energy of Cu_xIn_yS for superior photothermocatalytic CO_2 conversion to C_2H_4

Longlong Wang,[ab] Ruirui Wang,*[b] Shuang Wei,[b] Kexin Li,[b] Hasnain Nawaz,[b] Bin He,[b] Mengyue Li[b] and Ruixia Liu*[abc]

[a] Henan Institute of Advanced Technology, Zhengzhou University, Zhengzhou, 450001, P. R. China

[b] Beijing Key Laboratory of Solid State Battery and Energy Storage Process, CAS Key Laboratory of Green Process and Engineering, State Key Laboratory of Mesoscience and Engineering, Institute of Process Engineering, Innovation Academy for Green Manufacture, CAS, Beijing 100190, P. R. China

[c] Longzihu New Energy Laboratory, Zhengzhou Institute of Emerging Industrial Technology, Henan University, Zhengzhou 450000, P. R. China

*Corresponding authors:

Email address: wangruirui@ipe.ac.cn (Ruirui Wang), rxliu@ipe.ac.cn (Ruixia Liu)

Supplementary Figures

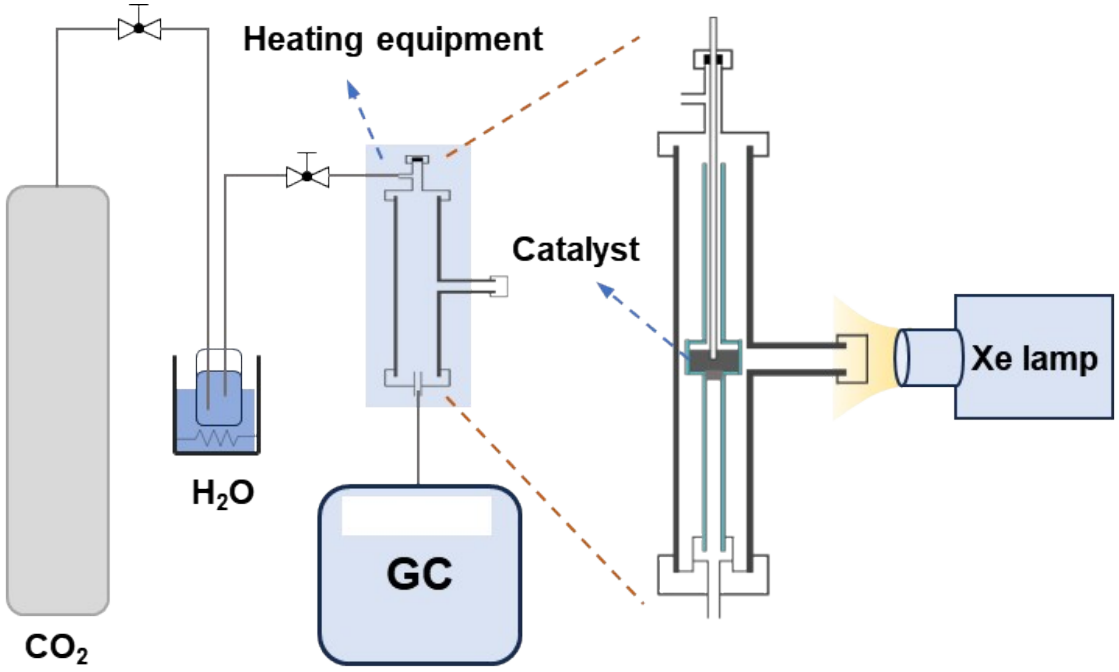

Fig. S1 Flow chart of reaction device.

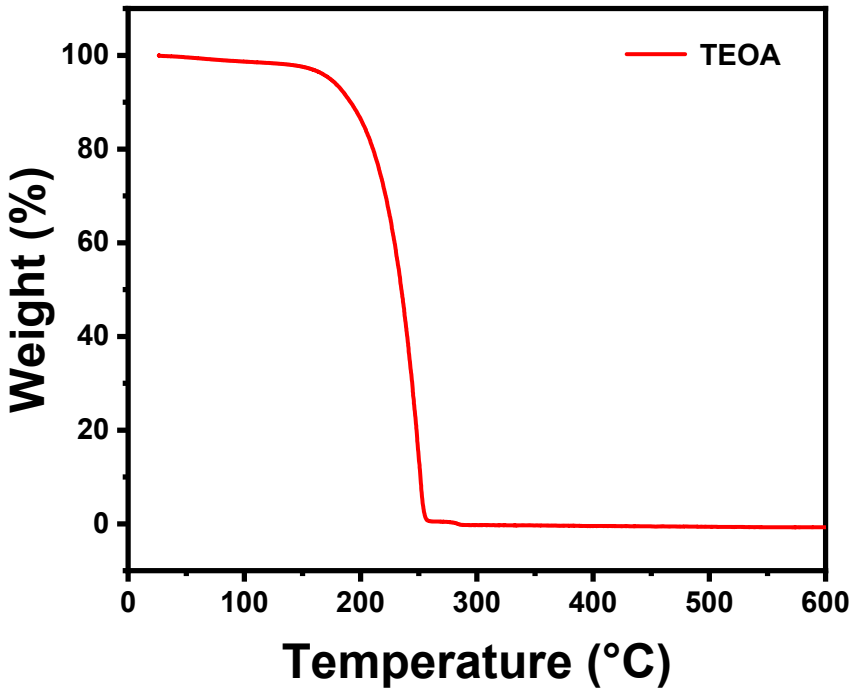

Fig. S2 Thermogravimetry graph of TEOA in nitrogen atmosphere.

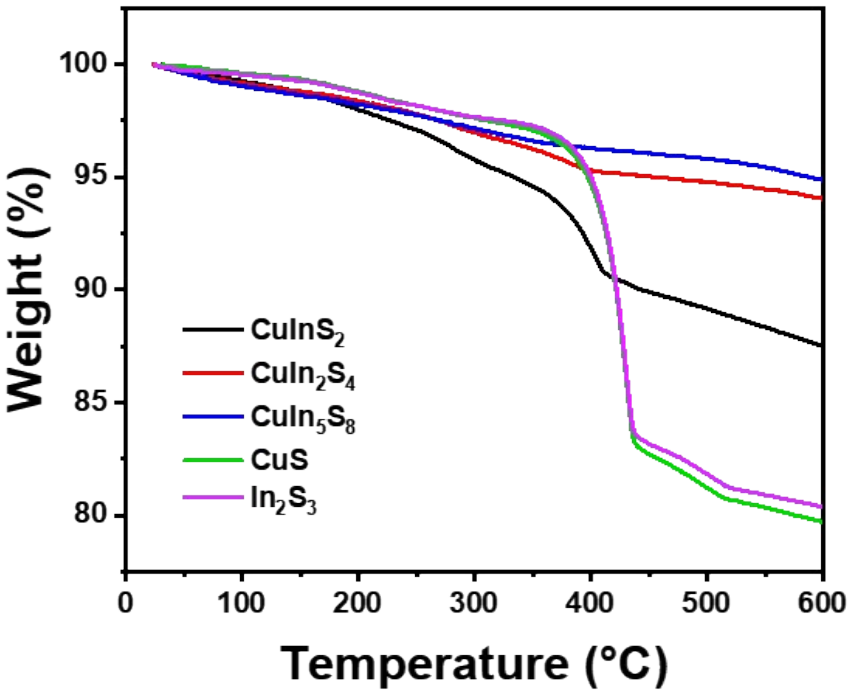

Fig. S3 Thermogravimetry graph of Cu_xIn_yS in nitrogen atmosphere.

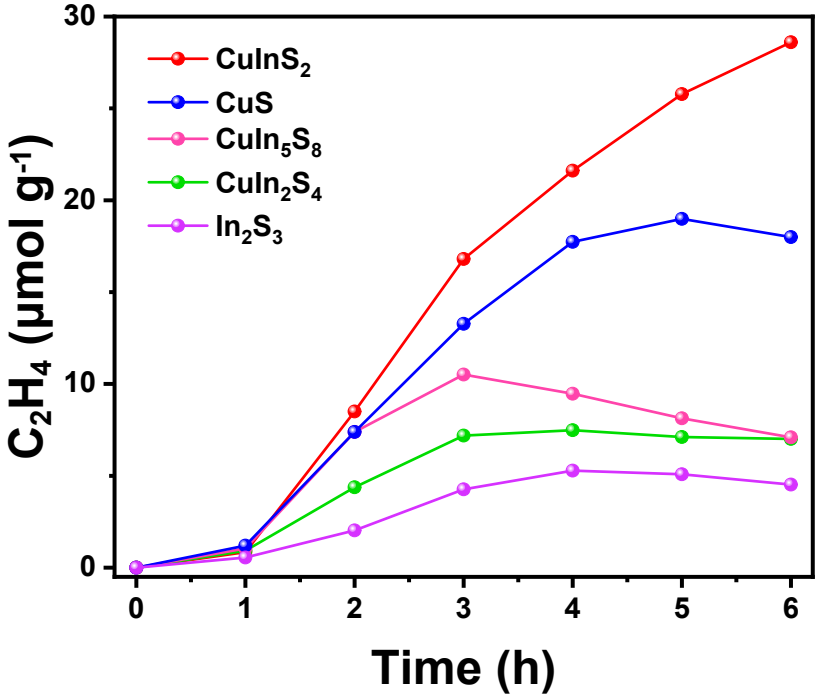

Fig. S4 Evolution of C_2H_4 yield over time for different samples.

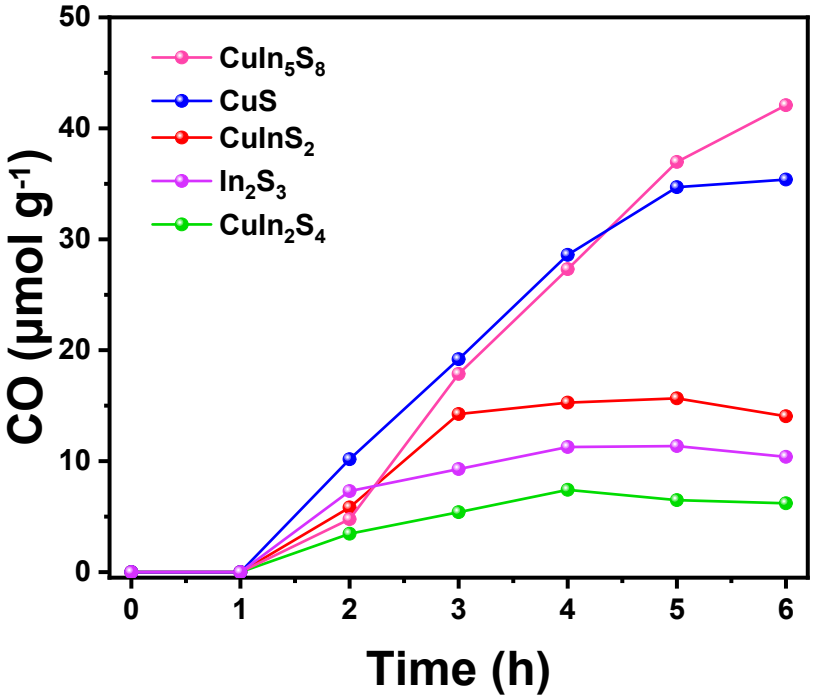

Fig. S5 Evolution of CO yield over time for different samples.

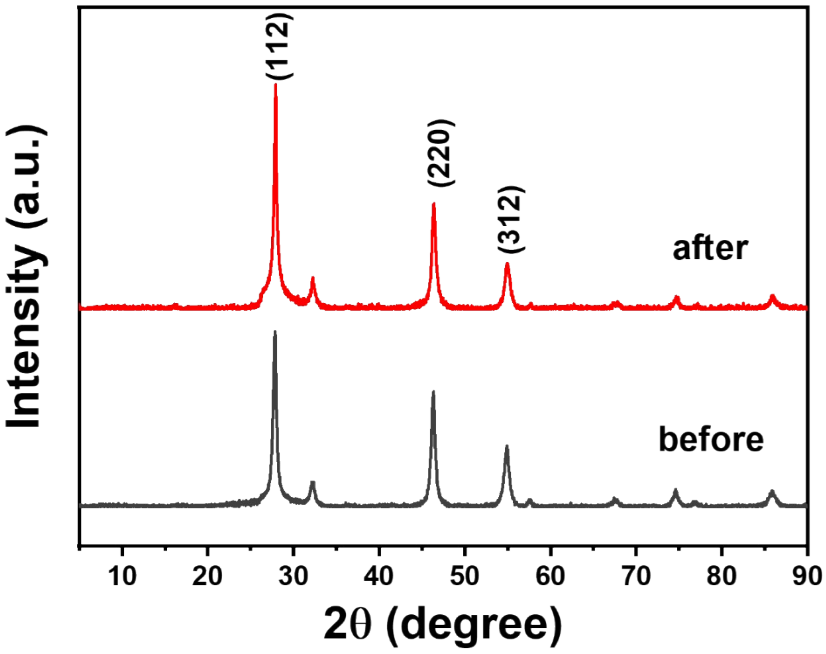

Fig. S6 XRD pattern of $CuInS_2$ sample before and after reaction.

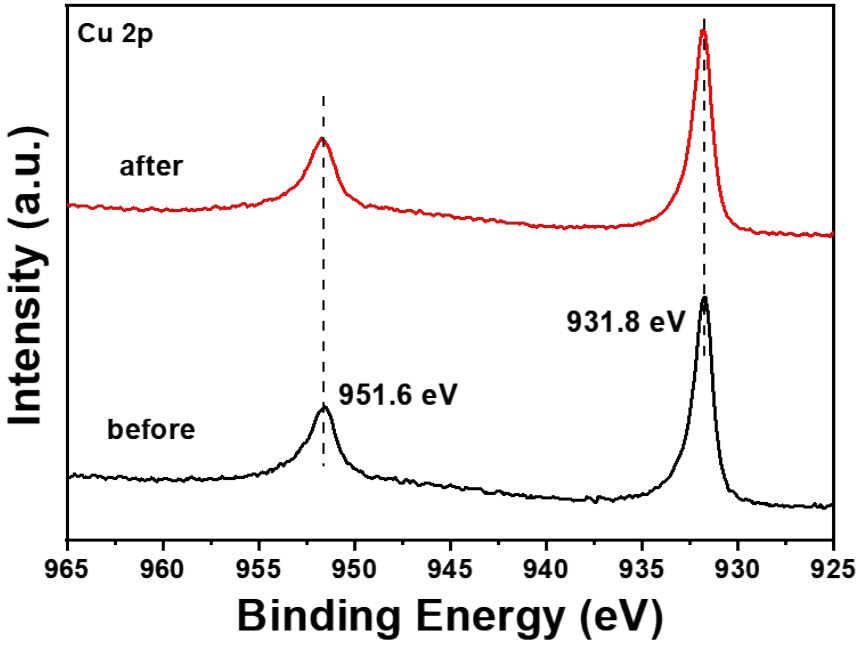

Fig. S7 XPS spectra before and after reaction for $CuInS_2$ sample: Cu 2p.

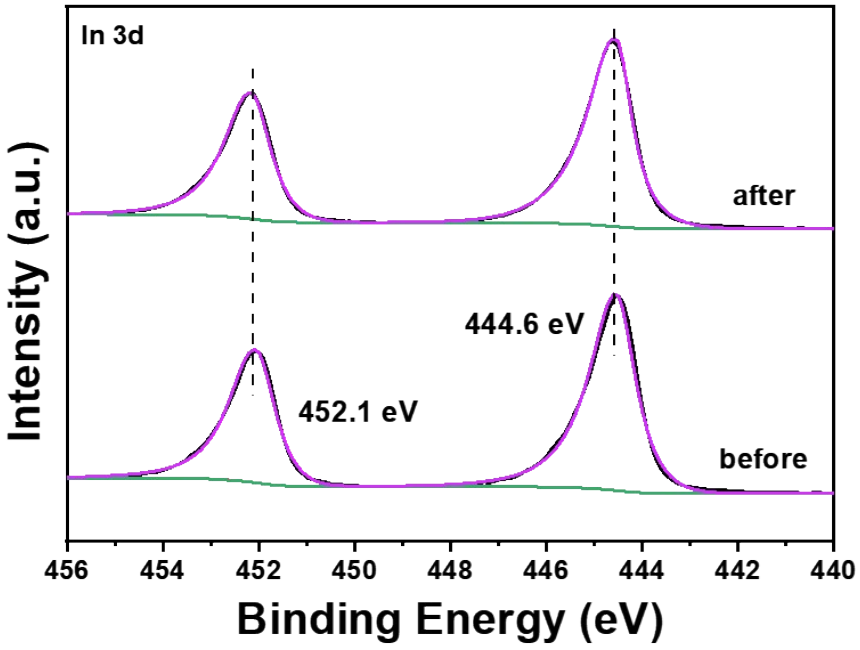

Fig. S8 XPS spectra before and after reaction for $CuInS_2$ sample: In 3d.

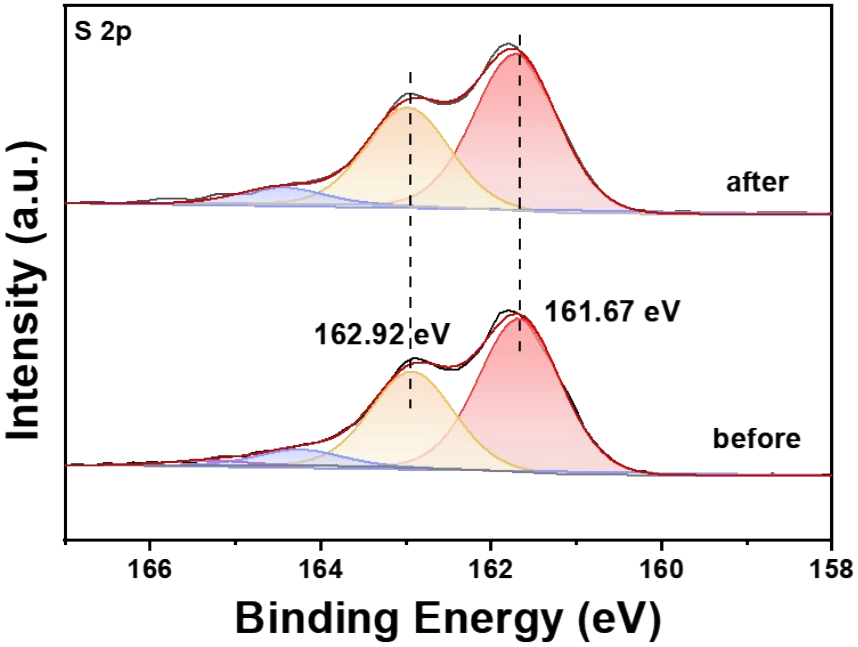

Fig. S9 XPS spectra before and after reaction for $CuInS_2$ sample: S 2p.

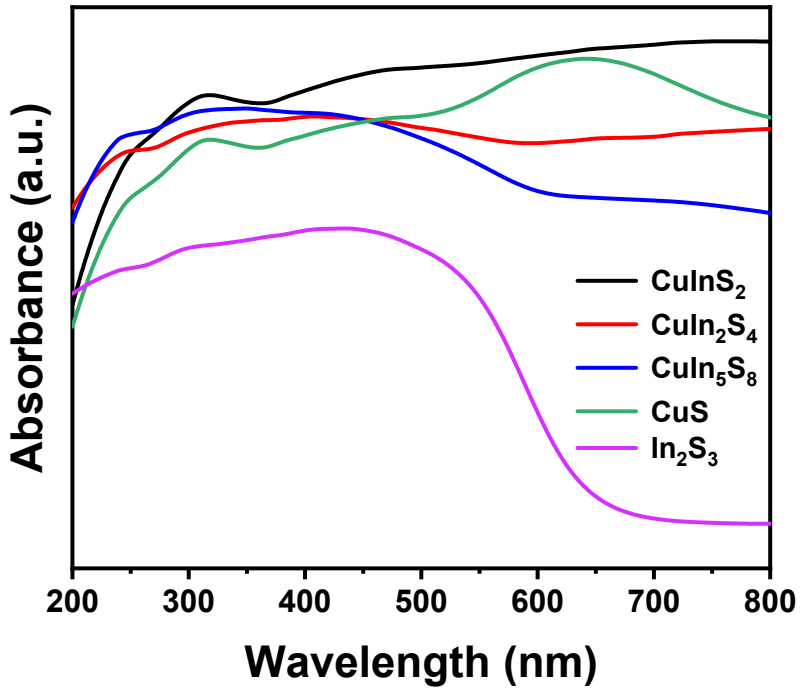

Fig. S10 UV-Vis absorption spectra of the Cu_xIn_yS.

Supplementary tables

Table S1 EDS mapping of the $CuInS_2$ sample.

Element	Atomic percent (%)
Cu	29.44
In	22.25
S	45.96
C	2.35
Total	100.00

Table S2 ICP-MS measurement of the $CuInS_2$ sample.

Sample	Quality m_0(g)	Elements of the test	Sample element content(W)
$CuInS_2$	0.01	Cu	35.40%
		In	31.30%

Table S3 Decomposition products of TEOA at 130 ℃ in nitrogen atmosphere.

Sample	C_2H_4/μmol g^{-1} h^{-1}	CO/μmol g^{-1} h^{-1}
TEOA	-	-

Table S4 Performance comparison of $CuInS_2$ and recently reported photothermal catalysts for C_2H_4 production

Catalyst	Reaction system	Light source	C_2H_4 production rate (μmol g^{-1} h^{-1})	C_2H_4 sel.%	Ref.
$CuInS_2$	CO_2+H_2O	300 W Xe lamp	45.7	79.7%	This work
CuO_X@p-ZnO	CO_2+H_2O	300 W Xe lamp	22.3	32%	[1]
$CuGaS_2$	CO_2+H_2	450 W Xe lamp with UV cut-off filter (KG-2 filter and CGA-400 filter)	20.1	77.2%	[2]
$CuInP_2S_6$	CO_2+H_2O	300 W Xe lamp	20.89	56.4%	[3]
BPQD – WO_3	CO_2+H_2O	300 W Xe lamp	11.0	13.5%	[4]
WO_{3-X}	CO_2+H_2O	300 W Xe lamp	1.3	34%	[5]
Sv-CdS@ZIF-8	CO_2+H_2O	300 W Xe lamp with a 420 nm cut-off filter	0.8	12.8%	[6]
CuACS/PCN	CO_2+H_2O	300 W Xe lamp	10.17	53.2%	[7]
Co-doped NiS_2 atomic layers	CO_2+H_2O	300 W Xe lamp with a AM1.5G filter	2.5	74.3%	[8]
WOTe	CO_2+H_2O	300 W Xe lamp	29.5	80%	[9]

Table S5 Photothermal catalytic CO_2 reduction performance in nitrogen and carbon dioxide atmospheres at 130 °C

Sample	C_2H_4/μmol g^{-1} h^{-1}	CO/μmol g^{-1} h^{-1}
$CuInS_2$+TEOA (N_2)	3.8	2.9
$CuInS_2$+TEOA (CO_2)	26.2	25.7

Reference

1 W. Wang, C. Deng, S. Xie, Y. Li, W. Zhang, H. Sheng, C. Chen and J. Zhao, Photocatalytic C-C coupling from carbon dioxide reduction on copper oxide with mixed-valence Copper(I)/Copper(II), *J. Am. Chem. Soc.*, 2021, **143**, 2984-2993.

2 S. Chakraborty, R. Das, M. Riyaz, K. Das, A. K. Singh, D. Bagchi, C. P. Vinod and S. C. Peter, Wurtzite $CuGaS_2$ with an In-situ-formed CuO layer photocatalyzes CO_2 conversion to ethylene with high selectivity, *Angew. Chem., Int. Ed.*, 2023, **62**, e202216613.

3 W. Gao, L. Shi, W. T. Hou, C. Ding, Q. Liu, R. Long, H. Q. Chi, Y. C. Zhang, X. Y. Xu, X. Y. Ma, Z. Tang, Y. Yang, X. Y. Wang, Q. Shen, Y. J. Xiong, J. L. Wang, Z. G. Zou and Y. Zhou, Tandem synergistic effect of Cu-In dual sites confined on the edge of monolayer $CuInP_2S_6$ toward selective photoreduction of CO_2 into multi-carbon solar fuels, *Angew. Chem., Int. Ed.*, 2024, **63**, e202317852.

4 W. Gao, X. Bai, Y. Gao, J. Liu, H. He, Y. Yang, Q. Han, X. Wang, X. Wu, J. Wang, F. Fan, Y. Zhou, C. Li and Z. Zou, Anchoring of black phosphorus quantum dots onto WO_3 nanowires to boost photocatalytic CO_2 conversion into solar fuels, *Chem. Commun.*, 2020, **56**, 7777-7780.

5 Y. Deng, J. Li, R. Zhang, C. Han, Y. Chen, Y. Zhou, W. Liu, P. K. Wong and L. Ye, Solar-energy-driven photothermal catalytic C-C coupling from CO_2 reduction over WO^{3-}, *Chin. J. Catal.*, 2022, **43**, 1230-1237.

6 F. Tian, H. Zhang, S. Liu, T. Wu, J. Yu, D. Wang, X. Jin and C. Peng, Visible-light-driven CO_2 reduction to ethylene on CdS: Enabled by structural relaxation-induced intermediate dimerization and enhanced by ZIF-8 coating, *Appl. Catal., B*, 2021, **285**, 119834.

7 W. Xie, K. Li, X. H. Liu, X. Zhang and H. Huang, P-mediated Cu-N_4 sites in carbon nitride realizing CO_2 photoreduction to C_2H_4 with selectivity modulation, *Adv. Mater.*, 2023, **35**, e2208132.

8 W. Shao, X. Li, J. Zhu, X. Zu, L. Liang, J. Hu, Y. Pan, J. Zhu, W. Yan, Y. Sun and Y. Xie, $Metal^{n+}$-$Metal^{\delta+}$ pair sites steer C-C coupling for selective CO_2 photoreduction to C_2 hydrocarbons, *Nano Research*, 2021, **15**, 1882-1891.

9 X. Zhang, Y. Yang, Y. Hu, L. Xiong, T. Wang, P. Li and J. Shen, Photothermal catalytic C-C coupling to ethylene from CO_2 with high efficiency by synergistic cooperation of oxygen vacancy and half-metallic WTe_2, *J. Energy Chem.*, 2024, **93**, 547-556.